

Cluster Ellipticities as a Cosmological Probe

Shirley Ho ¹, Neta Bahcall & Paul Bode

Department of Astrophysical Sciences, Princeton University, NJ 08544

ABSTRACT

We investigate the dependence of ellipticities of clusters of galaxies on cosmological parameters using large-scale cosmological simulations. We determine cluster ellipticities out to redshift unity for LCDM models with different mean densities Ω_m and amplitudes of mass fluctuation $\sigma_{8,0}$. The mean ellipticity increases monotonically with redshift for all models. Larger values of $\sigma_{8,0}$, i.e., earlier cluster formation time, produce lower ellipticities. The dependence of ellipticity on Ω_m is relatively weak in the range $0.2 \leq \Omega_m \leq 0.5$ for high mass clusters. The mean ellipticity $\bar{e}(z)$ decreases linearly with the amplitude of fluctuations at the cluster redshift z , nearly independent of Ω_m ; on average, older clusters are more relaxed and are thus less elliptical. The distribution of ellipticities about the mean is approximated by a Gaussian, allowing a simple characterization of the evolution of ellipticity with redshift as a function of cosmological parameters. At $z = 0$, the mean ellipticity of high mass clusters is approximated by $\bar{e}(z = 0) = 0.248 - 0.069\sigma_{8,0} + 0.013\Omega_{m,0}$. This relation opens up the possibility that, when compared with future observations of large cluster samples, the mean cluster ellipticity and its evolution could be used as a new, independent tool to constrain cosmological parameters, especially the amplitude of mass fluctuations, $\sigma_{8,0}$.

Subject headings: cosmology: theory — galaxies: clusters: general — large-scale structure of the universe

1. Introduction

Over the last twenty years the Cold Dark Matter (CDM) paradigm has become the standard model for structure formation in the Universe. It assumes the cosmic mass budget

¹E-mail: shirley@astro.princeton.edu

to be dominated by CDM, whose gravitational effects build structure from an initially Gaussian distribution of adiabatic fluctuations. Important parameters specifying CDM models include the fraction of the critical density in matter, Ω_m , and the fraction of the critical density in dark energy, Λ ; these in part determine the expansion rate of the universe and the shape of the initial matter power spectrum. Another important parameter is the amplitude of the power spectrum, conventionally quoted in terms of the rms linear mass fluctuation at $z = 0$ in a sphere of radius $8 h^{-1}\text{Mpc}$, $\sigma_{8,0}$ ($H_0 = 100h \text{ km s}^{-1}\text{Mpc}^{-1}$ throughout).

A series of exciting observations have been made in recent years which constrain these parameters, resulting in a concordance model (Bahcall et al. 1999; Spergel et al. 2003) — a spatially flat ΛCDM model with $\Omega_m \sim 0.25$. These include measurements of the cluster mass function, the strong cluster correlation function, and the evolution of the cluster abundance with redshift (Frenk et al. 1990; Bahcall & Cen 1992; Eke et al. 1998; Viana, Nichol & Liddle 2002; Bahcall et al. 2003; Bahcall & Bode 2003); the magnitude-redshift relation of Type Ia supernovae (Riess et al. 1999; Perlmutter et al. 1999); optical surveys of large scale structure (Eisenstein et al. 2005; Tegmark, Zaldarriga & Hamilton 2001; Pope et al. 2004; Cole et al. 2005); anisotropies in the cosmic microwave background (Bennett et al. 1996; Spergel et al. 2003); cosmic shear from weak lensing observations (van Waerbeke et al. 2001; Refregier 2003; van Waerbeke & Mellier 2005); and Lyman- α forest absorption (Croft, Hu & Dave 1999; McDonald, et al. 2004).

A key concept in the build-up of structure in this model is the formation of dark matter halos— quasi-equilibrium systems of dark matter, formed through non-linear gravitational collapse. Galaxies and other luminous objects are assumed to form by cooling and condensation of baryons within these halos (White & Rees 1978). Thus understanding the evolution and development of dark matter halos is an important step toward understanding structure formation. The possibility of using internal cluster properties to place constraints on cosmological parameters has been explored in a variety of ways. For example Richstone, Loeb & Turner (1992) suggested that the degree of substructure in clusters could constrain Ω_m . Different measures of substructure have been examined by Crone, Evrard & Richstone (1996) and Buote & Tsai (1995); the power ratio method of the latter has been applied to Chandra data by Jeltema et al. (2005), showing that clusters had more substructure in the past, but without setting any cosmological constraints.

An interesting property to investigate is the ellipticity or axis ratio of clusters. Observations suggest that cluster shapes, as traced by the distribution of galaxies (Plionis, Barrow & Frenk 1991; Rhee, van Haarlem & Katgert 1991; West & Bothun 1990; Strazzullo et al. 2005), X-ray emission and/or SZ decrement (McMillan, Kowalski & Ulmer 1989; Mohr et al. 1995; Kolokotronis et al. 2001; Wang & Fan 2004; De Filippis et al. 2005; Flores et al.

2005), and gravitational lensing (Oguri, Lee & Suto 2003; Hoekstra, Yee & Gladders 2004; Mandelbaum et al. 2005), are usually not spherical. There is some indication that the mean ellipticity is evolving with redshift (Melott, Chambers, & Miller 2001; Plionis 2002). Dark matter and hydrodynamic simulations have also been utilized, resulting in cluster-sized halos which are triaxial (West, Dekel & Oemler 1989; Evrard et al. 1993; de Theije, Katgert & van Kampen 1995; Splinter et al. 1997; Buote & Xu 1997; Jing & Suto 2002; Floor et al. 2003; Suwa et al. 2003; Ho & White 2004; Rahman et al. 2004; Flores et al. 2005; Hopkins, Bahcall & Bode 2005; Kasun & Evrard 2005; Allgood et al. 2005).

In this paper, we investigate the possibility of using cluster ellipticities as a cosmological probe, in particular of Ω_m and $\sigma_{8,0}$. The observed cluster samples are currently too small and too poorly characterized for strong constraints to be developed. However, with the ongoing optical, X-ray, weak lensing and SZ surveys providing an ever-increasing sample of clusters (e.g. Bahcall et al. 2003; Miller et al. 2005; Boehringer et al. 2004; Carlstrom, Holder & Reese 2002; Ruhl et al. 2004; Schwan et al. 2003; Kosowsky 2003) it will become possible to make more accurate statistical inferences concerning cluster ellipticities. In this paper we provide predictions of cluster ellipticities and their evolution for different cosmologies that could be directly compared with observations. We use numerical simulations of structure formation to generate clusters and determine their ellipticity evolution with redshift from $z = 0$ to $z = 1$, systematically varying Ω_m and $\sigma_{8,0}$ in order to understand how these parameters affect cluster structure. The simulations, cluster selection, and derivation of cluster ellipticity are presented in §2. The results of cluster ellipticities are shown in §3, and we conclude in §4.

2. Predicted cluster ellipticities

A series of N-body LCDM cosmological simulations were run, with the only differences between runs being in the matter density and the power spectrum amplitude; these were set to $\Omega_m = 0.2, 0.3, \text{ and } 0.5$, with $\sigma_{8,0} = 0.7, 0.9, \text{ and } 1.1$, for nine models in all. The linear CDM power spectrum was generated using the `lingers.f` code from the GRAFIC2¹ package (Bertschinger 2001), with a Hubble constant $h = 0.7$, baryon density $\Omega_b = 0.041$, and spectral index $n = 1$. GRAFIC2 was then used to generate the initial particle conditions, with the modification that the Hanning filter was not used because it suppresses power on small scales (McDonald, Trac & Contaldi 2005). All of the runs contained $N = 256^3$ particles in a periodic cube of size $500h^{-1}\text{Mpc}$, making the particle mass $m_p = 2.07 \times 10^{12}\Omega_m h^{-1}M_\odot$.

¹Available at <http://arcturus.mit.edu/grafic/>

Simulations were carried out using the TPM² code (Bode & Ostriker 2003) with a 512^3 mesh and a spline softening length of $20.35h^{-1}\text{kpc}$. The initial domain decomposition parameters in the TPM code were $A = 1.9$ and $B = 8.0$ (TPM was modified slightly so that there was no lower limit to B when it is reduced at later times, which improves the tracking of low mass halos; for details on these parameters see Bode & Ostriker (2003)).

The particle positions were saved for every expansion factor interval 0.1 between $a = 0.5$ and $a = 1$, i.e. from $z = 1$ to the present. The FOF (friends-of-friends) halo finder was run on each saved redshift, with a linking length $b = 0.164$ times the mean interparticle separation (Lacey & Cole 1994; Jenkins et al. 2001). The resulting mass functions were in good agreement with the predictive formula of Jenkins et al. (2001) (using $b = 0.164$) for halos with 32 or more particles (or mass above $3.3 \times 10^{13}h^{-1}M_{\odot}$ for $\Omega_m = 0.5$). The center of mass of each FOF halo thus identified was calculated, and all particles in a cube of size $4h^{-1}\text{Mpc}$ around this point were extracted. The most bound particle in this cube was identified, and all the particles within $1h^{-1}\text{Mpc}$ of this particle were selected to compute the ellipticity. All cluster ellipticities in this paper will refer to the ellipticity within a comoving radius of $1h^{-1}\text{Mpc}$, as this radius should be easier to determine observationally. Only halos with mass above $4 \times 10^{13}h^{-1}M_{\odot}$ (39 particles for $\Omega_m = 0.5$) within the $1h^{-1}\text{Mpc}$ radius were considered. Varying b from 0.14 to 0.2 had little effect on the final masses and ellipticities, because once a cluster center is chosen we use the mass within a specific radius of $1h^{-1}\text{Mpc}$. The same set of random phases was used for all the runs; we experimented with varying the seed used to generate these phases, and found this had no impact on the results. Current observations indicate that the dark matter radial profile of clusters, obtained by gravitational lensing observations, follows the galaxy radial profile on the scale of $1h^{-1}\text{Mpc}$ (Fischer & Tyson 1997; Carlberg et al. 1997). It is therefore expected that the observed distribution of galaxies will closely reflect the underlying mass distribution. The underlying mass distribution is also reflected in the observed distribution of the intracluster gas (for a recent review see Arnaud 2005). Further observations will shed additional light on this comparison.

To determine the ellipticity of a cluster, we find the best-fit ellipse using the matrix of second moments of particle positions about the center of mass:

$$I_{ij} = \sum m_p x_i x_j \quad (1)$$

where the sum is over all the particles selected in the manner just described. Given the normalized eigenvalues of I , λ_i , we use a common measure of ellipticity:

$$\epsilon = 1 - \sqrt{\lambda_2/\lambda_1} = 1 - a_2/a_1 \quad (2)$$

²Available at <http://astro.princeton.edu/~bode/TPM/>

where $\lambda_1 > \lambda_2 > \lambda_3$, and a_1 and a_2 are the primary and secondary ellipsoid axes' lengths respectively. Since the 3-D ellipticity is not directly measured in observations, we also measure the projected 2-D cluster ellipticities on the x-y plane. The process of determining the projected cluster ellipticities is repeated as above and the 2-D ellipticity of each halo is:

$$\epsilon_{2d} = 1 - \sqrt{\lambda_{2d,2}/\lambda_{2d,1}} \quad (3)$$

where $\lambda_{2d,2} > \lambda_{2d,1}$. This 2-D ellipticity will be our definition of ellipticities in the paper, unless otherwise specified.

After selecting the clusters as described above, we further separate the clusters into two groups: low mass clusters with masses $M_{1,0}$ in the range $4 \times 10^{13} \leq M_{1,0} < 10^{14} h^{-1} M_\odot$, and high mass clusters with $M_{1,0} \geq 10^{14} h^{-1} M_\odot$ ($M_{1,0}$ denotes the mass within $1 h^{-1} \text{Mpc}$). This division was made because the mean cluster ellipticities have a small mass dependence. Moreover, cluster surveys (including ACT, APEX, and SPT) which will produce larger cluster samples, will be best at detecting clusters with masses above $10^{14} h^{-1} M_\odot$ (Ruhl et al. 2004). As it would be challenging to have accurate measures of mass for a large number of clusters, we have investigated the effect of a 30% uncertainty in the mass determination in the threshold cut of $10^{14} h^{-1} M_\odot$; this change affected the resulting mean ellipticities by less than 3%.

3. Cluster Ellipticities and Structure Growth

In this section we investigate how cluster ellipticities depend upon the cosmological parameters Ω_m and $\sigma_{8,0}$. Fig. 1 presents the mean ellipticities as a function of redshift for high mass clusters ($M_{1,0} \geq 10^{14} h^{-1} M_\odot$). The error bars show the variance of the mean: $\sigma_e = N^{-1} \sqrt{\sum_i^N (e_i - \bar{e}(z))^2}$. The mean ellipticity increases with redshift for all models considered here. The dependence of cluster ellipticities on $\sigma_{8,0}$ is significant: higher $\sigma_{8,0}$ values (i.e. clusters are forming earlier) lead to lower ellipticities at $z = 0$. In contrast, the dependence on Ω_m is relatively weak.

An intriguing result is apparent in Fig. 2, which plots mean ellipticity at z , $\bar{e}(z)$, as a function of $\sigma_8(z)$: there is an inverse linear relation between the two, nearly independent of Ω_m (except indirectly in that $\sigma_8(z)$ depends on Ω_m). While the formation of clusters is a complex process, it appears that some average properties of clusters, such as ellipticities, can still be understood with a fairly simple picture: on average, the older the cluster, the more relaxed it is, and thus less elliptical. This is of course an over-simplified picture of the formation of clusters, but it does capture the general relation of Fig. 2. Based on this

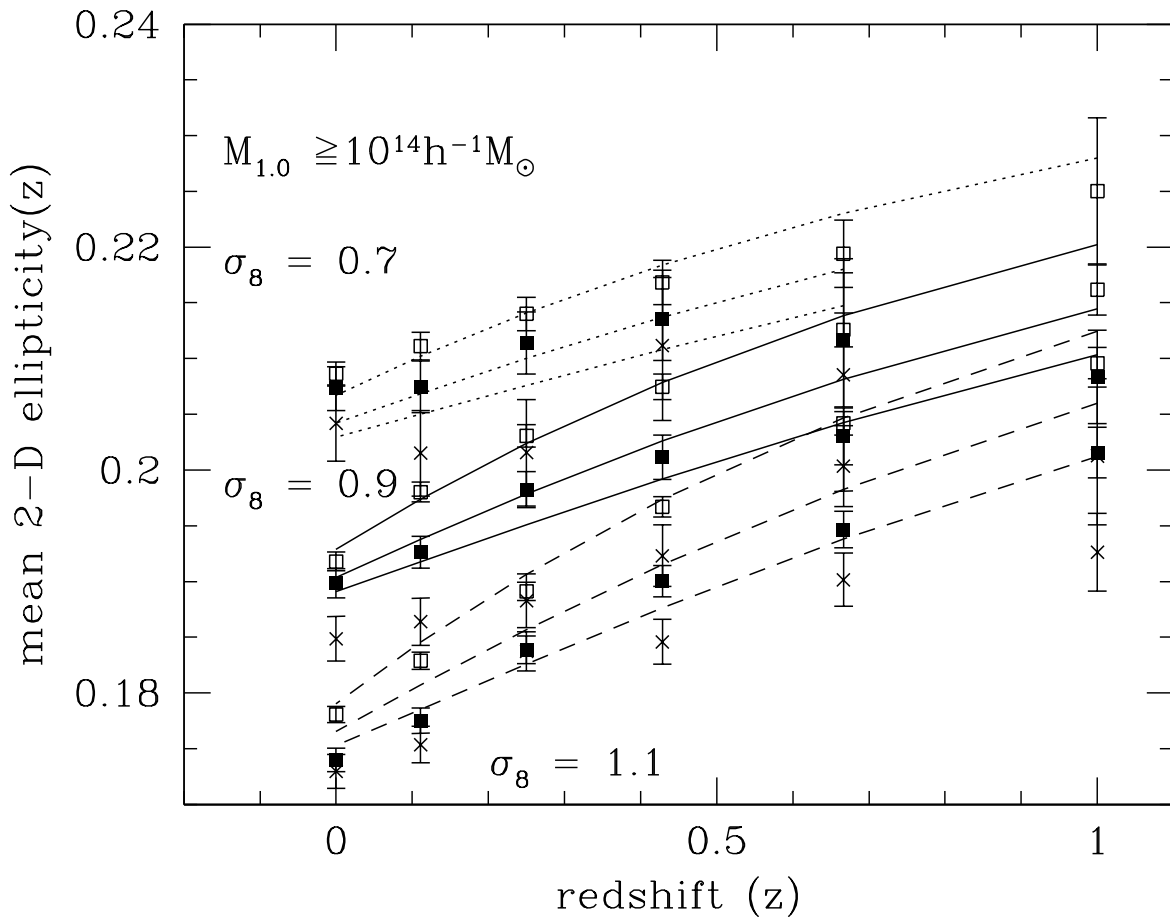


Fig. 1.— The evolution of mean cluster ellipticity (for $M_{1.0} \geq 10^{14} h^{-1} M_{\odot}$ clusters) as a function of redshift, for different models. The crosses represent $\Omega_m = 0.2$; solid squares represent $\Omega_m = 0.3$; empty squares $\Omega_m = 0.5$. The lines represent the corresponding fits from Eqn. 4: short-dash lines for $\sigma_{8,0} = 0.7$, solid lines for $\sigma_{8,0} = 0.9$, long-dash lines for $\sigma_{8,0} = 1.1$. Error bars are the variance of the mean.

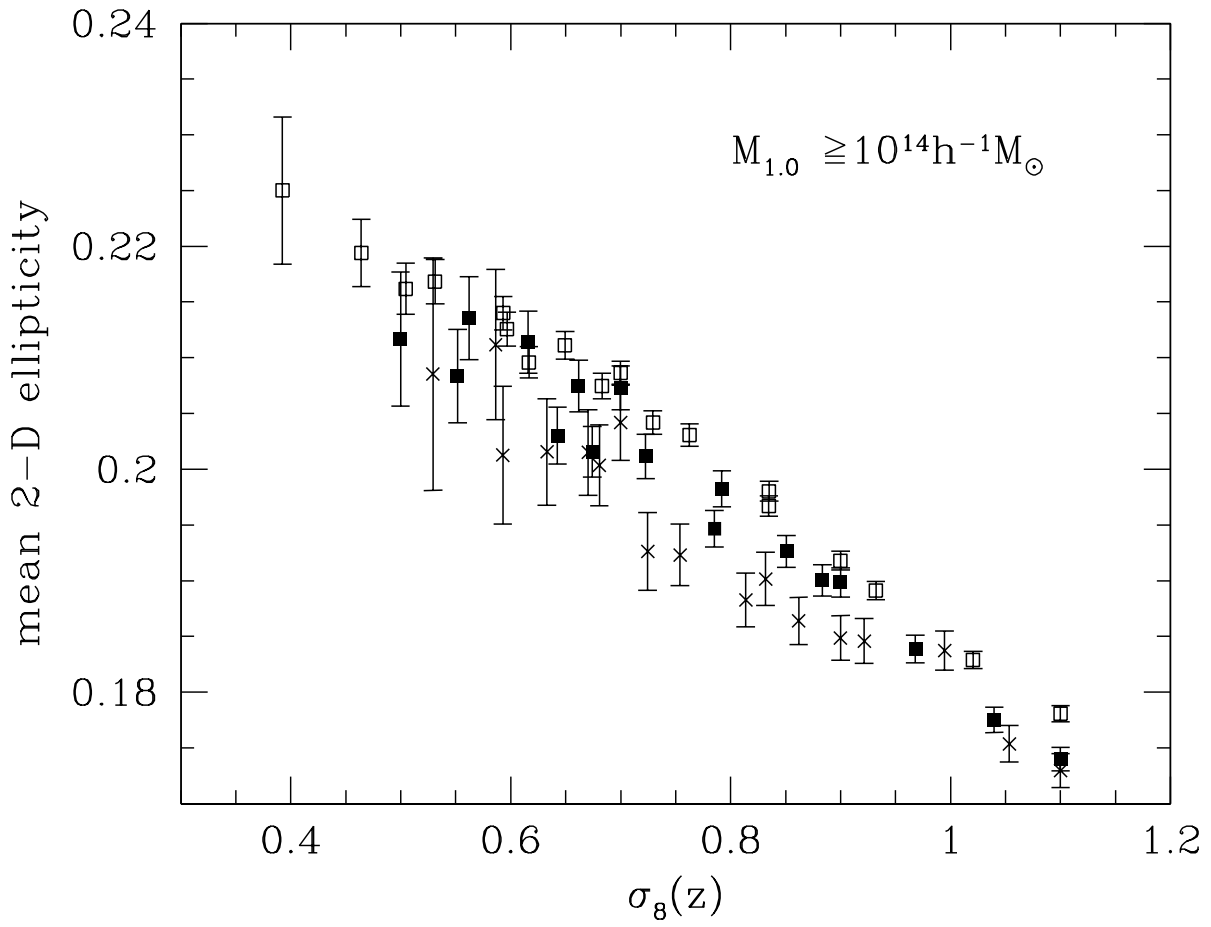


Fig. 2.— The mean cluster ellipticity $\bar{e}(z)$ at various redshifts $z \leq 1$, as a function of the linear $\sigma_8(z)$ (amplitude of mass fluctuations at redshift z). Point types denote different Ω_m , as in Fig. 1; all nine models are shown. Only clusters with $M_{1.0} \geq 10^{14} h^{-1} M_{\odot}$ are included.

Figure, we fit the mean ellipticity $\bar{e}(z)$ of the high mass clusters ($M_{1.0} \geq 10^{14} h^{-1} M_{\odot}$) to the following linear relationship:

$$\bar{e}(z) = 0.248 \left(1 - 0.250 \frac{\sigma_8(z)}{0.9} + 0.016 \frac{\Omega_m}{0.3} \right) \quad (4)$$

At $z = 0$ this relation becomes $\bar{e}(z = 0) = 0.248 - 0.069\sigma_{8,0} + 0.013\Omega_{m,0}$. This relation of ellipticity as a function of redshift is shown by the lines in Fig. 1. While there are small variations from model to model, the general trends are followed.

The distribution of ellipticities can be fit reasonably well by a Gaussian for all $z \leq 1$. For high mass clusters, the standard deviation is nearly the same for all runs: a value of $\sigma = 0.09$ is within ten percent of the value measured at any redshift for all the models. Thus, using the mean from Eqn. 4, it is possible to characterize the complete distribution of ellipticities out to $z = 1$. Also, as mentioned earlier, we have investigated including a 30% uncertainty in the mass determination in the cut at $10^{14} h^{-1} M_{\odot}$; this did not affect the resulting mean ellipticities at more than 3%.

The results for cluster ellipticities of low mass clusters ($4 \times 10^{13} \leq M_{1.0} < 10^{14} h^{-1} M_{\odot}$) are presented in Figures 3 and 4. These Figures demonstrate that the low mass clusters show the same trend of increasing ellipticity with redshift, as well as increasing ellipticity with decreasing $\sigma_{8,0}$. However the dependence on Ω_m is stronger than for the higher mass clusters. The fit corresponding to Eqn. 4 for these clusters is:

$$\bar{e}(z) = 0.238 \left(1 - 0.273 \frac{\sigma_8(z)}{0.9} + 0.107 \frac{\Omega_m}{0.3} \right) \quad (5)$$

While the dependence on Ω_m is more important for these smaller clusters, the dependence on $\sigma_8(z)$ is nearly the same for both samples: as with the higher mass clusters, for a given Ω_m , the ellipticity decreases as $\sigma_8(z)$ increases.

Different definitions of the mass of the cluster and different methods of measuring the axis ratio will change the measured value of the mean ellipticity. It has generally been found in simulations that less massive objects are rounder (e.g. Jing & Suto 2002; Hopkins, Bahcall & Bode 2005; Allgood et al. 2005). However, this assumes that the ellipticity is measured using a fixed overdensity or fraction of the virial radius; the outermost radius used thus becomes larger for more massive halos. Here we instead employ a fixed annular radius of $1 h^{-1} \text{Mpc}$, which is more suitable for direct comparison with observations. This radius is less than the virial radius for the largest clusters, while extending beyond the virial radius for less massive systems. Thus the low-mass sample, which includes more of the unrelaxed outlying regions of the clusters, actually has the same or a slightly higher mean ellipticity than the high-mass sample, where the relaxed cores dominate. Interestingly, Lee,

Jing & Suto (2005) derived an analytic prediction that more massive halos are less elliptical, but concluded there were conceptual difficulties in comparing their work to simulations, concerning precisely this issue of how the axis ratios are to be determined. It is of course important when comparing observations to simulations that the same definitions and methods be followed in the comparison.

4. Discussion and Conclusion

We use large-scale cosmological simulations to determine the mean ellipticity of clusters of galaxies and its evolution with redshift to $z = 1$, in order to investigate the possible use of this quantity as a new tool in constraining cosmological parameters. Nine LCDM cosmological models are studied, with Ω_m ranging from 0.2 to 0.5, and $\sigma_{8,0}$ ranging from 0.7 to 1.1. We provide predictions that can be directly compared with future observations of cluster ellipticities and can be used to place new independent constraints on cosmological parameters.

We find that the mean cluster ellipticity increases monotonically with redshift for all models. Clusters were more elliptical at earlier times. The mean ellipticity of high mass clusters ($M_{1.0} \geq 10^{14} h^{-1} M_\odot$) depends most strongly on $\sigma_{8,0}$: higher values of $\sigma_{8,0}$, i.e., earlier cluster formation times, produce lower ellipticities than lower $\sigma_{8,0}$ values. The dependence of ellipticity on Ω_m is relatively weak. The high mass clusters exhibit an interestingly regular behavior for all the LCDM models: the mean ellipticity $\bar{e}(z)$ depends linearly on $\sigma_8(z)$, the amplitude of fluctuations at the cluster redshift z . The effect of Ω_m is weak (in the range $0.2 \leq \Omega_m \leq 0.5$) for a given $\sigma_8(z)$. The distribution of ellipticities for these clusters can be described by a Gaussian, with a mean given by Eqn. 4 and a standard deviation of 0.09. This simple description can be used for direct comparison with observations, as well as for constraining the cosmological parameters, especially σ_8 . It can also be a useful input into the 'halo model' (Smith & Watts 1995) of large-scale structure.

The close connection between the mean ellipticity and $\sigma_8(z)$, suggests that clusters form with similar high ellipticities at formation time and thereafter undergo relaxation, becoming more spherical with time e.g., (e.g. Floor et al. 2003; Hopkins, Bahcall & Bode 2005; Allgood et al. 2005). The amplitude $\sigma_8(z)$ reflects the cluster formation time: larger amplitudes correspond to earlier cluster formation, and hence to a lower relative ellipticity at a given redshift. In a low density universe, furthermore, the merger rate is reduced at low redshift, allowing this relaxation to continue without much perturbation. Both the formation time of clusters and the merger rate are linked with the amplitude of the spectrum of mass fluctuations and hence with the ellipticity. However, the exact time of cluster

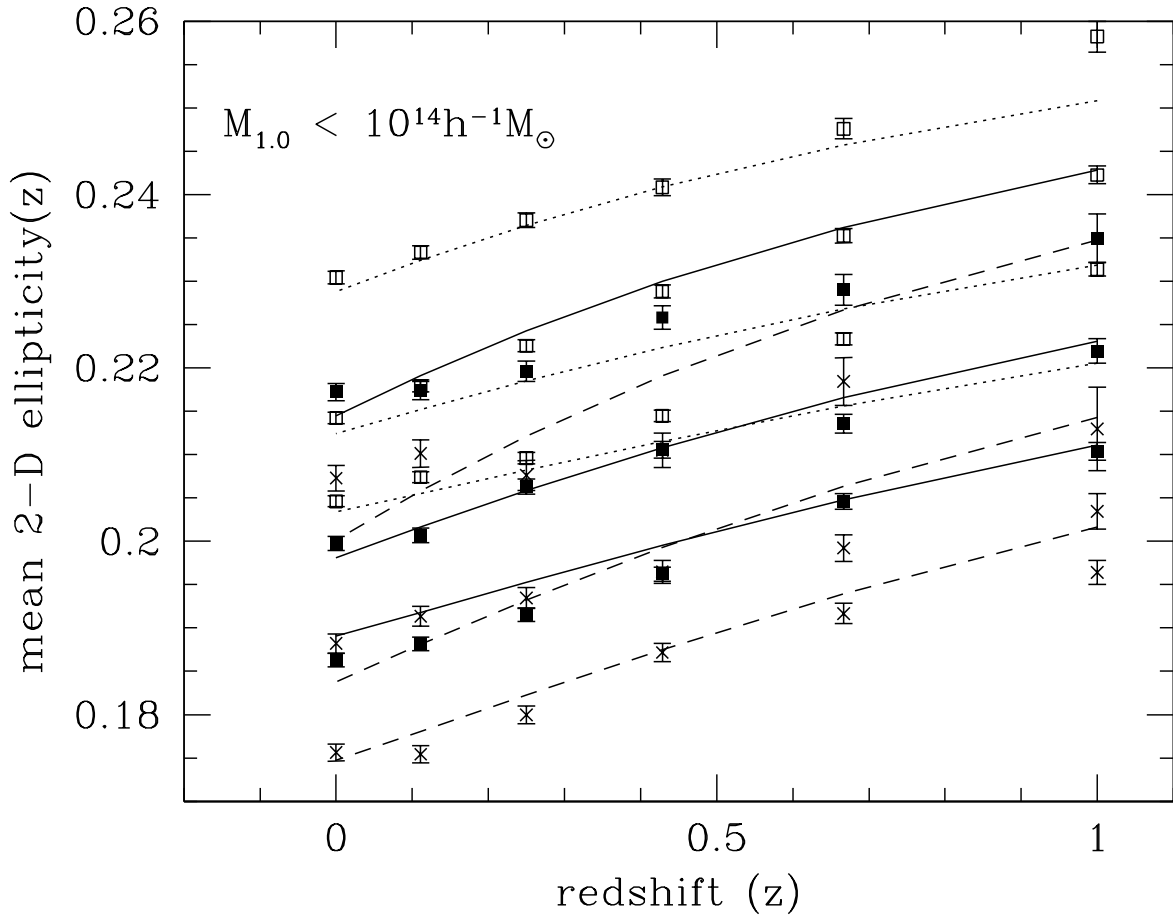


Fig. 3.— The evolution of mean cluster ellipticities, for low mass clusters. Point and line types as in Fig. 1

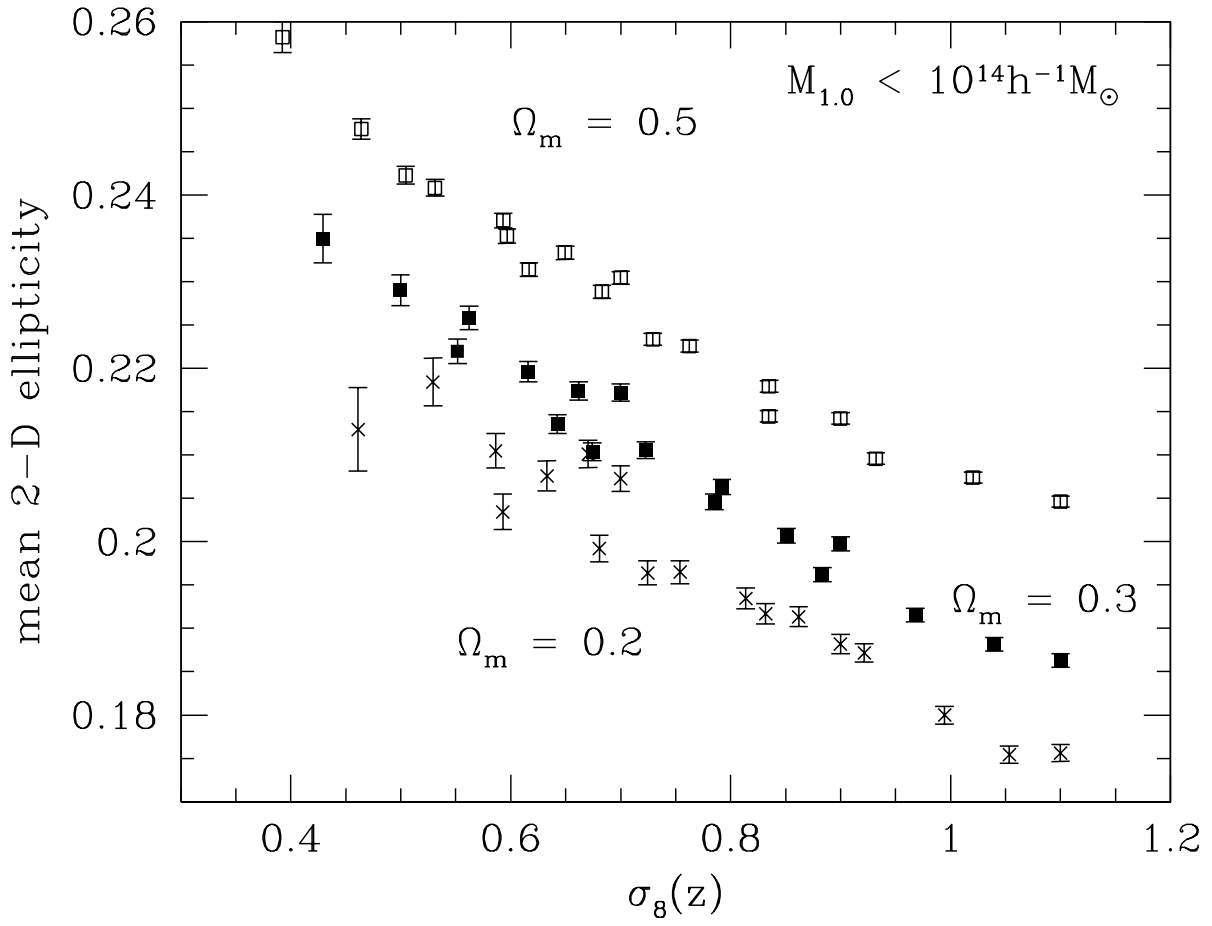


Fig. 4.— The evolution of $\bar{e}(z)$ for $4 \times 10^{13} h^{-1} M_\odot \leq M_{1.0} < 10^{14} h^{-1} M_\odot$, as a function of $\sigma_{8,0}$; point types as in Fig. 1.

formation cannot be easily defined (Cohn & White 2005), since a more accurate theoretical understanding of structure formation is necessary to explain the link.

Numerous large cluster surveys are currently underway or in planning stages, aimed at producing increasingly more accurate and complete samples of clusters. Such surveys will enable the determination of cluster ellipticities for large and complete cluster samples using the galaxy distribution (optical), the hot gas distribution (X-ray and SZ), and the dark matter distribution (lensing) in the clusters. These surveys include, among others, the Sloan Digital Sky Survey (Bahcall et al. 2003; Miller et al. 2005), the Red Sequence Cluster Survey (Gladders 2000), X-ray and SZ cluster surveys (Flores et al. 2005; Ruhl et al. 2004; Schwan et al. 2003), ACT (Kosowsky 2003), gravitational lensing surveys (Kaiser 2004), and LSST³. Each method has different selection functions and selection biases, as is well known. The ability to measure and compare cluster ellipticities using several independent methods will enable not only an improved understanding of the internal structure and physical processes in clusters, but will also enable the use of cluster ellipticities in cosmology.

The computations were run at Princeton on facilities supported by NSF grant AST-0216105, and at the National Center for Supercomputing Applications with support of a grant of supercomputing time (number MCA04N002P). This research was supported in part by Bahcall's NSF grant AST-0407305. We would like to thank Neal Dalal, Hy Trac, Joe Hennawi, Chris Hirata, Amol Upadhye, Feng Dong, and Mike Gladders for their helpful discussions.

REFERENCES

- Allgood, B., Flores, R.A., Primack, J.R., Kravtsov, A.V., Wechsler, R.H., Faltenbacher, A. & Bullock, J.S. 2005, MNRAS, submitted (astro-ph/0508497)
- Arnaud, M. 2005, Proc. Enrico Fermi, International School of Physics Course CLIX, ed. F. Melchiorri & Y. Rephaeli (Washington, DC: IOS Press)
- Bahcall, N.A., Ostriker, J.P., Perlmutter, S. & Steinhardt, P. 1999, Science, 284, 1481
- Bahcall, N.A., & Bode, P. 2003, ApJ, 588, 1
- Bahcall, N.A., & Cen, R. 1992 ApJ, 398, 81

³<http://www.lsst.org>

- Bahcall, N.A., et al. 2003, ApJ, 585, 182
- Bennett, C.L., Banday, A., Gorski, K.M., Hinshaw, G., Jackson, P., Keegstra, P., Kogut, A., Smoot, G.F., Wilkinson, D.T., Wright, E.L. 1996, ApJ, 464, L1-L4
- Bertschinger, E. 2001, ApJS, 137, 1
- Bahcall, N. et al. 2003 ApJS, 148, 243
- Bode, P. & Ostriker, J.P. 2003, ApJS, 145, 1
- Boehringer, H., Schuecker, P., Guzzo, L., Collins, C.A., Voges, W., Cruddace, R.G., Ortiz-Gil, A., Chincarini, G., De Grandi, S., Edge, A.C., MacGillivray, H.T., Neumann, D.M., Schindler, S. & Shaver, P. 2005, A&A, 425, 367
- Buote, D.A. & Tsai, J.C. 1995, ApJ, 452, 522
- Buote, D.A. & Xu, G. 1997, MNRAS, 284, 439
- Carlberg, R.G., Yee, H.K.C., & Ellingson, E. 1997, ApJ, 478, 462
- Carlstrom, J.E., Holder, G.P. & Reese, E.D. 2002, ARA&A, 40, 643
- Cohn, J.D., White, M. 2005, APh, in press (astro-ph/0506213)
- Cole, S. et al. 2005, MNRAS, in press (astro-ph/0501174)
- Croft, R. A. C., Hu, W., Dave, R. 1999, Phys. Rev. Lett., 83, 1092
- Crone, M.M., Evrard, A.E. & Richstone, D.O. 1996, ApJ, 467, 489
- Eisenstein et al. 2005 , ApJ, submitted, (astro-ph/0501171)
- Eke, V.R., Cole, S., Frenk, C.S., Petrick Henry, J. 1998, MNRAS, 298, 1145
- Evrard, A.E., Mohr, J.J., Fabricant, D.G. & Geller, M.J. 1993, ApJ, 419, L9
- De Filippis, E., Sereno, M., Bautz, M.W. & Longo, G. 2005, ApJ, 625, 108
- Fischer, P. & Tyson, J. A. 1997, AJ, 114, 14
- Floor, S. N., Melott, A. L., Miller, C. J., & Bryan, G. L. 2003, ApJ, 591, 741
- Flores, R.A., Allgood, B., Kravtsov, A.V., Primack, J.R., Buote, D.A. & Bullock, J.S. 2005, MNRAS, submitted (astro-ph/0508226)

- Frenk, C.S., White, S.D.M., Efstathiou, G., Davis, M. 1990, *ApJ*, 351, 10
- Gladders, M.D. 2000, *Bulletin of the American Astronomical Society*, 32, 1499
- Hallman, E.J., Motl, P.M., Burns, J.O. & Norman, M.L. 2005, *ApJ*, submitted (astro-ph/0509460)
- Ho, S., White, M. 2004, *APh*, 24, 257
- Hoekstra, H., Yee, H.K.C., Gladders, M. 2004, *ApJ*, 606, 67
- Hopkins, P.F., Bahcall, N.A., & Bode, P. 2005, *ApJ*, 618, 1
- Jeltema, T.E., Canizares, C.R., Bautz, M.W. & Buote, D.A. 2005, *ApJ*, 624, 606
- Jenkins, A., Frenk, C.S., White, S.D.M., Colberg, J.M., Cole, S., Evrard, A.E. & Yoshida, N. 2001, *MNRAS*, 321, 372
- Jing, Y.P. & Suto, Y. 2002, *ApJ*, 574, 538
- Kaiser, N. 2004 *Proceedings of the SPIE*, 5489, 11
- Kasun, S.F. & Evrard, A.E. 2005, *ApJ*, 629, 781
- Kolokotronis, V., Basilakos, S., Plionis, M. & Georgantopoulos, I. 2001, *MNRAS*, 320, 49
- Kosowsky, A. 2003, *New Astronomy Reviews*, 47, 939
- Lacey, C. & Cole, S. 1994, *MNRAS*, 271, 676
- Lee, J., Jing, Y.P. & Suto, Y. 2005, *ApJ*, 632, 706
- Mandelbaum, R., Hirata, C., Broderick, T., Seljak, U., Brinkmann, J. 2005, *MNRAS*, submitted (astro-ph/0507108)
- McDonald, P., Seljak, U., Burles, S., Schlegel, D. J., Weinberg, D. H., Shih, D., Schaye, J., Schneider, D. P., Brinkmann, J., Brunner, R. J., Fukugita, M. 2004, astro-ph/0405013
- McDonald, P., Trac, H. & Contaldi, C. 2005, *ApJ*, submitted (astro-ph/0505565)
- McMillan, S.L.W., Kowalski, M.P. & Ulmer, M.P. 1989, *ApJS*, 70, 723
- Melott, A. L., Chambers, S. W., & Miller, C. J. 2001, *ApJ*, 559, L75
- Miller, C.J. et al. 2005, *AJ*, 130, 968

- Mohr, J.J., Evrard, A.E., Fabricant, D.G. & Geller, M.J. 1995, ApJ, 447, 8
- Oguri, M., Lee, J. & Suto, Y. 2003, ApJ, 599, 7
- Paz, D.J., Lambas, D.G., Padilla, N. & Merchan, M. 2005, MNRAS, submitted (astro-ph/0509062)
- Perlmutter, S. et al. 1999, ApJ, 517, 565
- Plionis, M. 2002, ApJ, 572, L67
- Plionis, M., Barrow, J.D., & Frenk, C.S. 1991, MNRAS, 249, 662
- Pope, A.C., et al. 2005, ApJ, 607, 655
- Rahman, N., Shandarin, S.F., Motl, P.M. & Melott, A.L. 2004, MNRAS, submitted (astro-ph/0405097)
- Refregier, A. 2003, ARA&A41, 645
- Rhee, G.F.R.N., van Haarlem, M.P. & Katgert, P. 1991, A&AS, 91, 513
- Richstone, D., Loeb, A. & Turner, E.L. 1992, ApJ, 393, 477
- Riess, A.B., et al. 1998, Phys. Rev. D, 37, 3406
- SPT collaboration: Ruhl, J.E. et al. 2004, Proc. SPIE, 5498, 11
- Schulz, A.E., Hennawi, J. & White, M. 2005, preprint (astro-ph/0508118)
- Smith, R.E. & Watts, P.I.R. 2005, MNRAS, 360, 203
- Spergel, D.N., Verde, L., Peiris, H.V. Komatsu, E., Nolta, M.R., Bennett, C.L., Halpern, M., Hinshaw, G., Jarosik, N., Kogut, A., Limon, M. Meyer, S.S., Page, L., Tucker, G.S., Welland, J.L., Wollack, E. & Wright, E.L. 2003, ApJS, 148, 175
- Splinter, R.J., Melott, A.L., Linn, A.M., Buck, C. & Tinker, J. 1997, ApJ, 479, 632
- Strazzullo, V., Paolillo, M., Longo, G., Puddu, E., Djorgovski, S.G., De Carvalho, R.R. & Gal, R.R. 2005, MNRAS, 359, 191
- Suwa, T., Habe, A., Yoshikowa, K. & Okamoto, T. 2003, ApJ, 588, 7
- Schwan, D. et al. 2003, New Astronomy Reviews 47, 993
- Tegmark, M., Zaldarriga, M., & Hamilton, A., J. 2001, Phys. Rev. D, 63, 43007

- de Theije, P.A.M., Kartgert, P. & van Kampen, E. 1995, MNRAS, 273, 30
- van Waerbeke, L., Mellier, Y., Radovich, M., Bertin, E., Dantel-Fort, M., McCracken, H.J.,
Le Fevre, O., Foucaud, S., Cuillandre, J.-C., Erben, T., Jain, B., Schneider, P.,
Bernardeau, F. & Fort, B. 2001, A&A, 374, 757
- van Waerbeke, L. & Mellier, Y. 2005, Gravitational Lensing Impact on Cosmology, IAU
Symposium 225, ed. Y. Mellier & G. Meylan (Cambridge, UK: Cambridge University
Press), 3
- Viana, P.T.P., Nichol R.C., & Liddle A.R. 2002, ApJ569, 75
- Wang, Y.-G. & Fan, Z.-H. 2004, ApJ, 617, 847
- West, M.J. & Bothun, G.D. 1990, ApJ, 350, 36
- West, M.J., Dekel, A., & Oemler, A. 1989, ApJ, 336, 46
- White, S. D. M., Rees, M. J. 1978 MNRAS, 183, 341